

# A kinematic approach to Kokotsakis meshes

Hellmuth Stachel<sup>1</sup>

*Institute of Discrete Mathematics and Geometry, Vienna University of Technology,  
Wiedner Hauptstr. 8-10/104, A 1040 Wien, Austria*

---

## Abstract

A Kokotsakis mesh is a polyhedral structure consisting of an  $n$ -sided central polygon  $\mathcal{P}_0$  surrounded by a belt of polygons in the following way: Each side  $a_i$  of  $\mathcal{P}_0$  is shared by an adjacent polygon  $\mathcal{P}_i$ , and the relative motion between cyclically consecutive neighbor polygons is a spherical coupler motion. Hence, each vertex of  $\mathcal{P}_0$  is the meeting point of four faces. In the case  $n = 3$  the mesh is part of an octahedron.

These structures with rigid faces and variable dihedral angles were first studied in the thirties of the last century. However, in the last years there was a renaissance: The question under which conditions such meshes are infinitesimally or continuously flexible gained high actuality in discrete differential geometry. The goal of this paper is to revisit the wellknown continuously flexible examples (Bricard, Graf, Sauer, Kokotsakis) from the kinematic point of view and to extend their list by a new family.

*Keywords:* Kokotsakis mesh, discrete conjugate net, overconstrained mechanism, spherical coupler motion

---

## 1. Introduction

The definition of a Kokotsakis mesh (German: Neunflach) dates back to A.I. Kokotsakis (1932). While for arbitrary  $n$  the classification of *continuously flexible* Kokotsakis meshes is an open problem (compare Bobenko et al., 2008, p. 76), for the case  $n = 3$  we know since R. Bricard (1897) that there are three flexible types (see also Stachel, 1987).

In discrete differential geometry there is an interest in polyhedral structures composed of quadrilaterals, i.e., in *quadrilateral surfaces*. When all quadrilaterals are planar, the edges form a *discrete conjugate net* (see, e.g., Pottmann et al., 2007, Fig. 14e). When each quadrilateral is seen as a rigid body and only the dihedral angles can vary, the question arises under which conditions such structures are flexible. In Bobenko et al. (2008), p. 75, the following theorem

---

<sup>1</sup>*Email address:* [stachel@dmg.tuwien.ac.at](mailto:stachel@dmg.tuwien.ac.at),  
*URL:* <http://www.dmg.tuwien.ac.at/stachel>

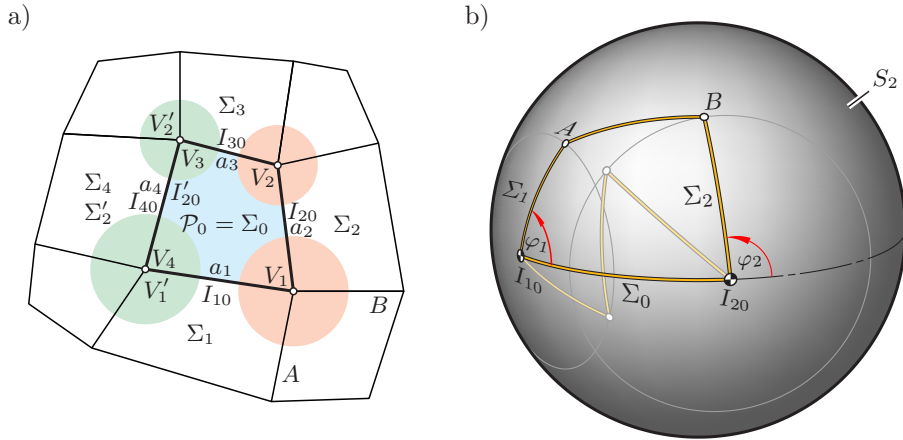


Figure 1: a) Kokotsakis mesh for  $n = 4$  and b) spherical image of the pyramide with apex  $V_1$

can be found:

*A discrete conjugate net is continuously flexible if and only if all its  $3 \times 3$  complexes, i.e., all included Kokotsakis meshes, are continuously flexible.*

This reveals the recent interest in these examples of overconstrained structures.

### 1.1. Kinematic interpretation

Let us concentrate on the case  $n = 4$  (see Fig. 1a). In terms of kinematics the involved polygons  $\mathcal{P}_0, \dots, \mathcal{P}_4$  represent different *systems*  $\Sigma_0, \dots, \Sigma_4$ , i.e., rigid bodies. The central polygon  $\mathcal{P}_0$  with vertices  $V_1, \dots, V_3$  and sides  $a_1, \dots, a_4$  stands for the fixed system  $\Sigma_0$ . The sides  $a_i$  are instantaneous axes  $I_{i0}$  of the relative motions  $\Sigma_i/\Sigma_0$ , i.e., of  $\Sigma_i$  against  $\Sigma_0$ .

For  $n = 4$  the edges of a Kokotsakis mesh constitute a net of *folds*. There are four connected triples of edges. For the sake of brevity, we call them *horizontal* or *vertical* (note Fig. 1a). The horizontal folds include either  $a_1$  or  $a_3$  as central edge, the vertical folds pass either through  $a_2$  or through  $a_4$ . Each vertex  $V_i$  is a crossing point of a horizontal and a vertical fold.

Since not the lengths of the sides  $a_1 = \overline{V_1V_2}, \dots, a_4 = \overline{V_4V_1}$  of  $\mathcal{P}_0$ , but only their directions have an influence on the flexibility, we can translate all four-sided pyramids with apex  $V_i$ ,  $i = 1, \dots, 4$ , through a common center  $O$ . If we intersect these pyramids with the unit sphere  $S_2$  centered at  $O$ , we obtain the *spherical image* of the mesh. Then we can state:

**Theorem 1.** *A Kokotsakis mesh is of  $k$ -th order infinitesimally flexible,  $k = 1, 2, \dots$ , or continuously flexible if and only if its spherical image is of  $k$ -th order infinitesimally or continuously flexible, respectively.*

First order infinitesimal flexibility of such meshes has been characterized by Kokotsakis (1932) and recently by O.N. Karpenkov (2008). It should be noted that due to B. Wegner (1984) first order flexibility of a spherical structure is

*equivalent* to first order flexibility of its planar sections; this principle called ‘coning’ is the main reason for the projective invariance of first order flexibility. 2nd order infinitesimal flexibility or Kokotsakis meshes has recently been studied in Bobenko et al. (2008).

If we intersect the planes adjacent to the vertex  $V_i$  with a sphere centered at  $V_i$ , the relative motion  $\Sigma_{i+1}/\Sigma_i$ ,  $i = 1, \dots, 4 \pmod{4}$ , is a spherical coupler motion. To recall, a *spherical coupler motion* (see Fig. 1b) is based on a spherical quadrangle  $I_{10}I_{20}BA$  with constant edge lengths but variable angles. It transmits the rotation about the center  $I_{10}$  through the angle  $\varphi_1$  by the coupler  $AB$  non-uniformly to the rotation about  $I_{20}$  through  $\varphi_2$ .

A Kokotsakis mesh is continuously flexible if and only if the transmission of the rotation  $\Sigma_1/\Sigma_0$  to  $\Sigma_3/\Sigma_0$  by the two coupler motions at  $V_1$  and  $V_2$  on the right hand side (Fig. 1a) is the same as via  $V_4$  and  $V_3$  on the left hand side. This is why we change the notation slightly and replace  $\Sigma_4, V_4, V_3, a_4 = I_{40}$  by  $\Sigma'_2, V'_1, V'_2, a'_2 = I'_{20}$ , respectively. Of course, in the flexible case there is also a two-fold ‘horizontal’ decomposition of the transmission  $\Sigma'_2/\Sigma_2$ , one via  $\Sigma_1$  and the other via  $\Sigma_3$ .

The transference from a Kokotsakis mesh to its spherical image gives a unique result only if each edge is oriented. It is quite natural to endow the axes  $I_{10}, \dots, I_{40}$  with an orientation since the angles of rotations about these axes need to be signed. However, the orientation of all other edges — or, equivalently, the choice of half-edges terminated by  $V_i$  — is arbitrary. This leads to some ambiguities.

### 1.2. Known continuously flexible examples

Up to recent, to the author’s best knowledge the following examples of continuously flexible Kokotsakis meshes are known. Under appropriate notation and orientation of edges the flexible cases can be characterized as follows:

- (I) **Planar-symmetric** type (Kokotsakis, 1932, § 18): The reflection in the plane of symmetry of  $V_1$  and  $V_4$  maps each horizontal fold onto itself while the two vertical folds are exchanged.
- (II) **Translational** type: There is a translation  $V_1 \mapsto V_4$  and  $V_2 \mapsto V_3$  mapping the three planes on the right hand side onto the triple on the left hand side.
- (III) **Isogonal** type (Kokotsakis, 1932; Bobenko et al., 2008): At each vertex opposite angles are congruent. We return to this  $3 \times 3$  complex of a Voss surface in Section 4.1.
- (IV) **Orthogonal** type (Sauer, Graf, 1931; Sauer, 1970): Here the horizontal folds are located in parallel (say: horizontal) planes, the vertical folds in vertical planes.  $\mathcal{P}_0$  is a trapezoid. The underlying conditions for this  $3 \times 3$  complex of T-nets will be presented in Section 4.2.

In Section 4.3 a new family of continuously flexible Kokotsakis meshes will be introduced, which we call the **line-symmetric** type V though the symmetries

are only locally. This family includes Kokotsaki's remarkable example of a planar tessellation with congruent convex quadrangles (Kokotsakis (1932, Fig. 15), note also Bobenko et al. (2008, Fig. 8) or Stachel (2009)).

The famous Miura-ori folding technique (e.g., Piekarski (2000) or Stachel (2009)) contains  $3 \times 3$  complexes which are of type II, III and IV, simultaneously. As shown in Stachel (2000), any Cardan joint is also based on a spherical coupler motion, however a particular case where the sides  $I_{10}A$ ,  $I_{20}B$  and  $AB$  have the spherical length  $\pi/2$ . An appropriate combination of two Cardan joints gives a uniform transmission from  $\Sigma_1$  to  $\Sigma_3$ . This results in a flexible case with parallel axes  $I_{10}$  and  $I_{30}$  which obeys the conditions of type V; however, the second decomposition according to type V is no more a Cardan joint.

We finally emphasize that the complete classification of continuously flexible meshes has not been achieved yet.

### 1.3. Conventions

According to Theorem 1 our investigation takes place on the unit sphere  $S^2$  with center  $O$ . In order to avoid ambiguities in spherical geometry, we introduce the following notations and conventions:

- Each point  $A$  on the sphere has a diametrically opposed point  $\overline{A}$ , its *antipode*. A circle on  $S^2$  passing through  $A$  is a *great circle* if and only if it passes also through  $\overline{A}$ .
- For any two points  $A, B$  with  $B \neq A, \overline{A}$  the *spherical segment* or *bar*  $AB$  stands for the shorter of the two connecting arcs on the great circle spanned by  $A$  and  $B$ . We denote this great circle by  $[AB]$ .
- The *spherical distance*  $\overline{AB}$  is defined as the arc length of the segment  $AB$ . We require  $0 \leq \overline{AB} \leq \pi$  thus including also the limiting cases  $B = A$  and  $B = \overline{A}$ .
- The *oriented angle*  $\sphericalangle ABC$  on  $S^2$  is the angle of the rotation about axis  $OB$  which carries the segment  $BA$  into a position aligned with the segment  $BC$ . This angle is oriented in the mathematical sense, if looking from outside, and can be bounded by  $-\pi < \sphericalangle ABC \leq \pi$ .

## 2. Analysis of a spherical coupler motion

We start with the analysis of the spherical coupler motion, which is the spherical image of the flexing pyramide with apex  $V_1$  (Fig. 2): Let  $I_{10}I_{20}$  be the frame link of a spherical four-bar with the coupler  $A_1B_1$ . We denote the spherical length of the driving arm  $I_{10}A_1$  with  $\alpha_1$  and that of the driven arm  $I_{20}B_1$  with  $\beta_1$ . Furthermore, we set  $\gamma_1 := \overline{A_1B_1}$  and  $\delta_1 := \overline{I_{10}I_{20}}$  obeying

$$0 < \alpha_1, \beta_1, \gamma_1, \delta_1 < \pi.$$

The movement of the coupler remains unchanged when  $A_1$  is replaced by its antipode  $\overline{A_1}$  and at the same time  $\alpha_1$  and  $\gamma_1$  are substituted by  $\pi - \alpha_1$  and

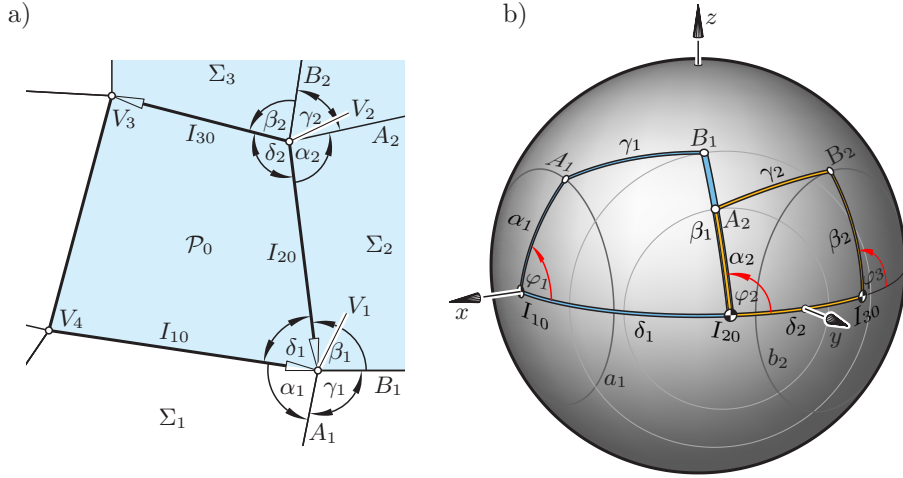


Figure 2: a) Pyramides with apices  $V_1$  and  $V_2$  and b) composition of the two spherical four-bars  $I_{10}A_1B_1I_{20}$  and  $I_{20}A_2B_2I_{30}$  with side lengths  $\alpha_i, \beta_i, \gamma_i, \delta_i, i = 1, 2$

$\pi - \delta_1$ , respectively. The same holds for the other vertices. When  $I_{10}$  is replaced by its antipode  $\bar{I}_{10}$ , then also the sense of orientation changes, when the rotation of the driving bar  $I_{10}A_1$  is inspected from outside of  $S^2$  either at  $I_{10}$  or at  $\bar{I}_{10}$ .

### 2.1. Relation between input and output angle

We use a cartesian coordinate frame with  $I_{10}$  on the positive  $x$ -axis and  $I_{10}I_{20}$  in the  $xy$ -plane such that  $I_{20}$  has a positive  $y$ -coordinate (see Fig. 2b). The input angle  $\varphi_1$  is measured between  $I_{10}I_{20}$  and the driving arm  $I_{10}A_1$  in mathematically positive sense. The output angle  $\varphi_2$  is the oriented exterior angle at vertex  $I_{20}$ , hence  $\varphi_2 = \sphericalangle \bar{I}_{10}I_{20}B_1$ . This results in the following coordinates:

$$A_1 = \begin{pmatrix} c\alpha_1 \\ s\alpha_1 c\varphi_1 \\ s\alpha_1 s\varphi_1 \end{pmatrix} \quad \text{and} \quad B_1 = \begin{pmatrix} c\beta_1 c\delta_1 - s\beta_1 s\delta_1 c\varphi_2 \\ c\beta_1 s\delta_1 + s\beta_1 c\delta_1 c\varphi_2 \\ s\beta_1 s\varphi_2 \end{pmatrix}.$$

Herein  $s$  and  $c$  are abbreviations for the sine and cosine function, respectively. In these equations the lengths  $\alpha_1, \beta_1$  and  $\delta_1$  are signed. The coordinates would also be valid for negative lengths.

The constant length  $\gamma_1$  of the coupler implies the condition

$$\begin{aligned} c\alpha_1 c\beta_1 c\delta_1 - c\alpha_1 s\beta_1 s\delta_1 c\varphi_2 + s\alpha_1 c\beta_1 s\delta_1 c\varphi_1 \\ + s\alpha_1 s\beta_1 c\delta_1 c\varphi_1 c\varphi_2 + s\alpha_1 s\beta_1 s\varphi_1 s\varphi_2 = c\gamma_1. \end{aligned} \quad (1)$$

Now we express  $s\varphi_i$  and  $c\varphi_i$  in terms of  $t_i := \tan \varphi_i/2$  setting

$$c\varphi = \frac{1 - t_i^2}{1 + t_i^2}, \quad s\varphi = \frac{2t_i}{1 + t_i^2}.$$

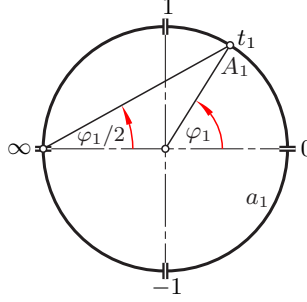


Figure 3:  $t_1 = \tan \varphi_1/2$  is a projective coordinate of point  $A_1$  on the circle  $a_1$

Note that  $t_1$  is a *projective coordinate* of point  $A_1$  on the circle  $a_1$  (see Fig. 3). The same is true for  $t_2$  and  $B_1 \in b_1$ . From (1) we obtain

$$\begin{aligned} & c\alpha_1 c\beta_1 c\delta_1 - c\alpha_1 s\beta_1 s\delta_1 \frac{1-t_2^2}{1+t_2^2} + s\alpha_1 c\beta_1 s\delta_1 \frac{1-t_1^2}{1+t_1^2} \\ & + s\alpha_1 s\beta_1 c\delta_1 \frac{1-t_1^2}{1+t_1^2} \frac{1-t_2^2}{1+t_2^2} + s\alpha_1 s\beta_1 \frac{2t_1}{1+t_1^2} \frac{2t_2^2}{1+t_2^2} = c\gamma_1 \end{aligned}$$

or

$$\begin{aligned} & -K(1+t_1^2)(1-t_2^2) + L(1-t_1^2)(1+t_2^2) + M(1-t_1^2)(1-t_2^2) \\ & + 4s\alpha_1 s\beta_1 t_1 t_2 + N(1+t_1^2)(1+t_2^2) = 0, \end{aligned} \quad (2)$$

where

$$\begin{aligned} K &= c\alpha_1 s\beta_1 s\delta_1, & M &= s\alpha_1 s\beta_1 c\delta_1, \\ L &= s\alpha_1 c\beta_1 s\delta_1, & N &= c\alpha_1 c\beta_1 c\delta_1 - c\gamma_1. \end{aligned} \quad (3)$$

The biquadratic equation (2) describes a *2-2-correspondence* between points  $A_1$  on circle  $a_1 = (I_{10}; \alpha_1)$  and  $B_1$  on  $b_1 = (I_{20}; \beta_1)$ . It can be abbreviated by

$$c_{22}t_1^2t_2^2 + c_{20}t_1^2 + c_{02}t_2^2 + c_{11}t_1t_2 + c_{00} = 0 \quad (4)$$

setting

$$\begin{aligned} c_{00} &= -K + L + M + N, & c_{02} &= K + L - M + N, \\ c_{11} &= 4s\alpha_1 s\beta_1 \neq 0, \\ c_{20} &= -K - L - M + N, & c_{22} &= K - L + M + N. \end{aligned} \quad (5)$$

Alternatively, (2) can also be expressed as

$$\begin{aligned} & \sin \frac{\alpha_1 - \beta_1 + \gamma_1 + \delta_1}{2} \sin \frac{\alpha_1 - \beta_1 - \gamma_1 + \delta_1}{2} t_1^2 t_2^2 \\ & + \sin \frac{\alpha_1 + \beta_1 + \gamma_1 + \delta_1}{2} \sin \frac{\alpha_1 + \beta_1 - \gamma_1 + \delta_1}{2} t_1^2 - 2 \sin \alpha_1 \sin \beta_1 t_1 t_2 \\ & + \sin \frac{\alpha_1 + \beta_1 + \gamma_1 - \delta_1}{2} \sin \frac{\alpha_1 + \beta_1 - \gamma_1 - \delta_1}{2} t_2^2 \\ & + \sin \frac{\alpha_1 - \beta_1 + \gamma_1 - \delta_1}{2} \sin \frac{\alpha_1 - \beta_1 - \gamma_1 - \delta_1}{2} = 0. \end{aligned} \quad (6)$$

*Remark:* It should be noted that conversely the 2-2-correspondance (4) defines  $\alpha_1, \dots, \delta_1$  uniquely. This can be seen as follows: First we get

$$\begin{aligned} 4K &= -c_{00} + c_{02} - c_{20} + c_{22}, & 4L &= c_{00} + c_{02} - c_{20} - c_{22}, \\ 4M &= c_{00} - c_{02} - c_{20} + c_{22}, & 4N &= c_{00} + c_{02} + c_{20} + c_{22}. \end{aligned}$$

On the other hand

$$\frac{4K}{c_{11}} = \frac{s\delta_1}{\tan \alpha_1}, \quad \frac{4L}{c_{11}} = \frac{s\delta_1}{\tan \beta_1}, \quad \frac{4M}{c_{11}} = c\delta_1, \quad \frac{4N}{c_{11}} = \frac{c\alpha_1 c\beta_1 c\delta_1 - c\gamma}{s\alpha_1 s\beta_1}.$$

This gives consecutively  $c\delta_1$ ,  $\tan \alpha_1$ ,  $\tan \beta_1$  and  $c\gamma_1$ , which defines the four bar-lengths uniquely within the interval  $[0, \pi]$ .

## 2.2. Relation between opposite angles

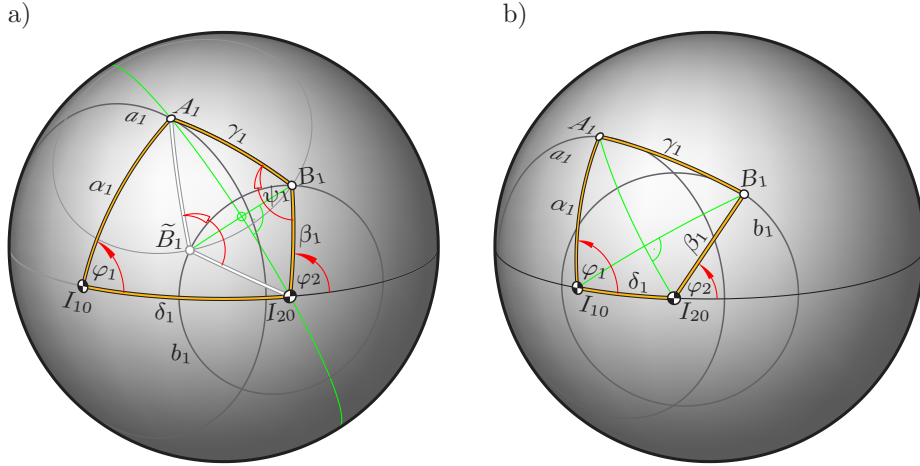


Figure 4: a) Opposite angles  $\varphi_1$  and  $\psi_1$  at the spherical four-bar  $I_{10}A_1B_1I_{20}$ ; b) Orthogonal case: each quadrangle has orthogonal diagonals

At the end of this analysis of a spherical four-bar mechanism we focus on opposite angles in the spherical quadrangle  $I_{10}A_1B_1I_{20}$ : The diagonal  $A_1I_{20}$  splits the quadrangle into two triangles, and we inspect the interior angles  $\varphi_1$  at  $I_{10}$  and  $\psi_1$  at  $B_1$  (Fig. 4a). Also for non-convex quadrangles, the spherical Cosine Theorem implies

$$\overline{\cos A_1I_{20}} = c\beta_1 c\gamma_1 + s\beta_1 s\gamma_1 c\psi_1 = c\alpha_1 c\delta_1 + s\alpha_1 s\delta_1 c\varphi_1$$

Hence there is a linear function, i.e., there are constants  $k_1, l_1 \in \mathbb{R}$  such that

$$c\psi_1 = k_1 + l_1 c\varphi_1 \quad \text{for} \quad -1 \leq c\psi_1, c\varphi_1 \leq 1 \quad (7)$$

with

$$k_1 = \frac{c\alpha_1 c\delta_1 - c\beta_1 c\gamma_1}{s\beta_1 s\gamma_1}, \quad l_1 = \frac{s\alpha_1 s\delta_1}{s\beta_1 s\gamma_1}. \quad (8)$$

For later use it is necessary to define also  $\psi_1$  as an oriented angle, hence

$$\psi_1 = \sphericalangle I_{20}B_1A_1, \quad \varphi_1 = \sphericalangle I_{20}I_{10}A_1 \quad \text{under} \quad -\pi < \psi_1, \varphi_1 \leq \pi.$$

This is still compatible with eq. (7).

We note that in general for given  $\varphi_1$  there are two positions  $B_1$  and  $\tilde{B}_1$  on circle  $b_1$  obeying (7). They are placed symmetrically with respect to the diagonal  $A_1I_{20}$ . So, the corresponding oriented angles  $\sphericalangle I_{20}B_1A_1$  and  $\sphericalangle I_{20}\tilde{B}_1A_1$  have different signs (Fig. 4a).

**Lemma 2.** *The cosines of the opposite oriented angles  $\psi_1 = \sphericalangle I_{20}B_1A_1$  and  $\varphi_1 = \sphericalangle I_{20}I_{10}A_1$  at the four-bar are linearly related by eq. (7). The signs of  $\varphi_1$  and  $\psi_1$  are different if and only if  $B_1$  and  $I_{10}$  are on different sides of  $[A_1I_{20}]$ .*

*Remark:* Contrary to the 2-2-correspondance describing the relation between  $\varphi_1$  and  $\varphi_2$ , the linear function (7) does not characterize the underlying four-bar uniquely. This follows immediately from a parameter count.

### 2.3. Particular cases

*Spherical isogram:*

Under the conditions  $\beta_1 = \alpha_1$  and  $\delta_1 = \gamma_1$  opposite sides of the quadrangle  $I_{10}A_1B_1I_{20}$  have equal lengths. Such quadrangles are called spherical *isograms*. In this case we have  $c_{00} = c_{22} = 0$  in (4), and eq. (6) converts into

$$s\alpha_1 [-2s\alpha_1 t_1 t_2 + s(\alpha_1 + \gamma_1) t_1^2 + s(\alpha_1 - \gamma_1) t_2^2] = 0.$$

The left hand side can be decomposed as

$$\begin{aligned} & s(\alpha_1 - \gamma_1) [s(\alpha_1 - \gamma_1) t_2^2 - 2s\alpha_1 t_1 t_2 + s(\alpha_1 + \gamma_1) t_1^2] \\ & = [s(\alpha_1 - \gamma_1)t_2 - (s\alpha_1 + s\gamma_1)t_1] [s(\alpha_1 - \gamma_1)t_2 - (s\alpha_1 - s\gamma_1)t_1] \end{aligned}$$

because of  $s^2\alpha_1 - s^2\gamma_1 = s(\alpha_1 + \gamma_1)s(\alpha_1 - \gamma_1)$ . *The 2-2-correspondance between the circles  $a_1$  and  $b_1$  splits into two projectivities*<sup>2</sup>

$$t_1 \mapsto t_2 = \frac{(s\alpha_1 \pm s\gamma_1)}{s(\alpha_1 - \gamma_1)} t_1, \quad (9)$$

provided  $\alpha_1 \neq \gamma_1, \pi - \gamma_1$ . Both projectivities keep  $t_1 = 0$  and  $t_1 = \infty$  fixed (Fig. 3). These parameters belong to the two *folded* positions, where the coupler  $A_1B_1$  is aligned with the frame link  $I_{10}I_{20}$ . In these positions a bifurcation is possible between the two projectivities. (Note that at the planar analogue one of these projectivities is the identity  $t_2 = t_1$  as  $I_{10}A_1B_1I_{20}$  is a parallelogram.)

*Orthogonal case:*

For a given point  $A_1 \in a_1$  the corresponding  $B_1, \tilde{B}_1 \in b_1$  are the points of intersection between the circles  $(A_1; \gamma_1)$  and  $b_1 = (I_{20}; \beta_1)$  (see Fig. 4a). Hence,  $B_1$  and  $\tilde{B}_1$  are located on a great circle perpendicular to the great circle  $[A_1I_{20}]$ .

---

<sup>2</sup>As mentioned above, the vertices of the moving quadrangle can be replaced by their antipodes without changing the motion. This is the reason why the same property also shows up under  $\beta_1 = \pi - \alpha_1$  and  $\delta_1 = \pi - \gamma_1$ . We will not mention this in the future but only refer to an ‘appropriate choice of orientations’.

Under the condition

$$\cos \alpha_1 \cos \beta_1 = \cos \gamma_1 \cos \delta_1. \quad (10)$$

the diagonals of the spherical quadrangle  $I_{10}A_1B_1I_{20}$  are orthogonal (Fig. 4b) as each of the products equals the products of cosines of the four segments on the two diagonals. Hence, under (10)  $B_1$  and  $\tilde{B}_1$  are always aligned with  $I_{10}$ , but also conversely, the two points  $A_1$  and  $\tilde{A}_1$  corresponding to  $B_1$  are aligned with  $I_{20}$ .

**Lemma 3.** *Under condition (10) the 2-2-correspondence between  $a_1$  and  $b_1$  maps pairs of points  $A_1 \in a_1$  spherically aligned with  $I_{20}$  onto pairs of points  $B_1 \in b_1$  which are spherically aligned with  $I_{10}$ . Corresponding great circles  $[I_{20}A_1]$  and  $[I_{10}B_1]$  are orthogonal (Fig. 4b).*

*Remark:* In the notation (4) this is characterized by  $\det \begin{pmatrix} c_{22} & c_{02} \\ c_{20} & c_{00} \end{pmatrix} = 0$ , because by (5) this is equivalent to  $\det \begin{pmatrix} K & N \\ M & -L \end{pmatrix} = 0$ , which means

$$\alpha_1 \alpha_1 s\beta_1 c\beta_1 s^2\delta_1 + \alpha_1 \alpha_1 s\beta_1 c\beta_1 c^2\delta_1 - \alpha_1 s\beta_1 c\gamma_1 c^2\delta_1 = 0$$

or

$$\alpha_1 \alpha_1 s\beta_1 c\beta_1 = \alpha_1 s\beta_1 c\gamma_1 c\delta_1 \quad \text{under} \quad \alpha_1 s\beta_1 \neq 0.$$

### 3. Composition of two spherical coupler motions

Now we use the output angle  $\varphi_2$  of this coupler motion as the input angle of a second coupler motion with vertices  $I_{20}A_2B_2I_{30}$ , with arm lengths  $\alpha_2$ ,  $\beta_2$ , with the coupler length  $\gamma_2$  and with  $\delta_2$  as length of the frame link (Fig. 2b). The two frame links are assumed in aligned position. In the case  $\sphericalangle I_{10}I_{20}I_{30} = \pi$  the length  $\delta_2$  is positive, otherwise negative. Analogously, a negative  $\alpha_2$  expresses the fact that the aligned bars  $I_{20}B_1$  and  $I_{20}A_2$  are pointing to opposite sides. Changing the sign of  $\beta_2$  means replacing the output angle  $\varphi_3$  by  $\varphi_3 - \pi$ . The sign of  $\gamma_2$  has no influence on the transmission.

Due to (4) the transmission between the angles  $\varphi_1$ ,  $\varphi_2$  and the output angle  $\varphi_3$  of the second four-bar with  $t_3 := \tan \varphi_3/2$  can be expressed by the two biquadratic equations

$$\begin{aligned} c_{22}t_1^2t_2^2 + c_{20}t_1^2 + c_{02}t_2^2 + c_{11}t_1t_2 + c_{00} &= 0 \\ d_{22}t_2^2t_3^2 + d_{20}t_2^2 + d_{02}t_3^2 + d_{11}t_2t_3 + d_{00} &= 0. \end{aligned}$$

The  $d_{ik}$  are defined by equations analogue to eqs. (5) and (3). We eliminate  $t_2$  by computing the *resultant* of the two polynomials with respect to  $t_2$  and obtain

$$\det \begin{pmatrix} c_{22}t_1^2 + c_{02} & c_{11}t_1 & c_{20}t_1^2 + c_{00} & 0 \\ 0 & c_{22}t_1^2 + c_{02} & c_{11}t_1 & c_{20}t_1^2 + c_{00} \\ d_{22}t_3^2 + d_{20} & d_{11}t_3 & d_{02}t_3^2 + d_{00} & 0 \\ 0 & d_{22}t_3^2 + d_{20} & d_{11}t_3 & d_{02}t_3^2 + d_{00} \end{pmatrix} = 0. \quad (11)$$

This biquartic equation expresses a 4-4-*correspondance* between points  $A_1$  and  $B_2$  on the circles  $a_1$  and  $b_2$ , respectively.

#### 4. Examples of flexible Kokotsakis meshes

As mentioned above, a continuously flexible Kokotsakis mesh for  $n = 4$  is based on a two-fold decomposition of the transmission  $\Sigma_1 \rightarrow \Sigma_3$  into two spherical four-bars. In view of Fig. 1a we speak of the *right-hand decomposition* via  $\Sigma_2$  and the *left-hand decomposition* via  $\Sigma_4 = \Sigma'_2$ . Of course, in the translational type II the two decompositions have identical spherical images.

##### 4.1. Combination of isograms

When two isograms are combined, both 2-2-correspondances split into projectivities  $t_1 \mapsto t_2$  and  $t_2 \mapsto t_3$  with  $0 \mapsto 0$  and  $\infty \mapsto \infty$  in the sense of Fig. 3. Hence, also the 4-4-correspondance is composed from such projectivities. Each of them is uniquely defined by any pair  $t_1 \mapsto t_3$  with  $t_1 \neq 0, \infty$ . Beside the two isograms on the right-hand side we can also combine two isograms with lengths  $\alpha'_1, \dots, \delta'_1$  on the left-hand side such that both 4-4-correspondances share one projectivity. This proves the continuous flexibility of the *isogonal* type III: Any Kokotsakis mesh consisting of four *isogonal* pyramides — the preimages of spherical isograms — and with any given non-coplanar initial position is continuously flexible (Kokotsakis, 1932).

These arguments are not only true for  $n = 4$ . We can conclude that — referring to Fig. 1a — for  $k \geq 2$  isogonal pyramides on the ‘right-hand side’ of the central polygon  $\mathcal{P}_0$  and  $l \geq 1$  isogonal pyramides on the ‘left-hand side’ with a non-coplanar initial position a flexible Kokotsakis mesh arises with an  $n$ -sided central polygon,  $n = k + l$ . This includes for  $n = 3$  the Bricard octahedra of type 3. By (9) we can formulate the closure conditions as

$$\prod_{i=1}^k \frac{(s\alpha_i \pm s\gamma_i)}{s(\alpha_i - \gamma_i)} = \prod_{j=1}^l \frac{(s\alpha'_j \pm s\gamma'_j)}{s(\alpha_j - \gamma_j)} \quad \text{and} \quad \sum_{i=1}^k \delta_i = \sum_{j=1}^l \delta'_j$$

for any appropriate choice of signs.

##### 4.2. Combination of quadrangles with orthogonal diagonals

In view of Lemma 3 we combine two orthogonal four-bars such that they have one diagonal in common (see Fig. 5a), i.e., under  $\alpha_2 = \beta_1$  and  $\delta_2 = -\delta_1$ , hence  $I_{30} = I_{10}$ . Then the 4-4-correspondance between  $A_1$  and  $B_2$  is the square of the 2-2-correspondance

$$c_{21}t_1^2t_3 + c_{12}t_1t_3^2 + c_{10}t_1 + c_{01}t_3 = 0$$

which expresses the fact that  $A_1$  and  $B_2$  are permanently spherically aligned with  $I_{20}$ . The coefficients are

$$\begin{aligned} c_{21} &= t\beta_2(t\alpha_1 + t\delta_1), & c_{12} &= -t\alpha_1(t\beta_2 + t\delta_1), \\ c_{10} &= t\alpha_1(t\beta_2 - t\delta_1), & c_{01} &= -t\beta_2(t\alpha_1 - t\delta_1). \end{aligned}$$

Herein  $t$  is the abbreviation for the tangent function.

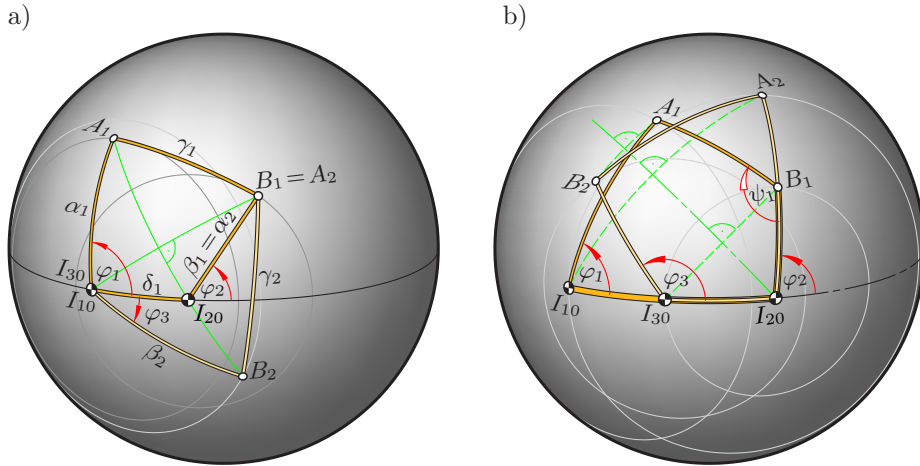


Figure 5: Spherical images of the right-hand decomposition a) of the orthogonal type IV, and b) of the line-symmetric type V

Obviously, any other composition of two such four-bars obeying

$$t\alpha'_1 : t\delta'_1 : t\beta'_2 = t\alpha_1 : t\delta_1 : t\beta_2 \quad (12)$$

gives the same transmission  $\varphi_1 \mapsto \varphi_3$ . This causes the flexibility of the  $(3 \times 3)$ -complexes included in T-nets, first studied in Sauer, Graf (1931). The spherical images of the horizontal folds are located on the great circle  $[I_{10}B_1]$ , that of the vertical folds on the orthogonal diagonals  $[I_{20}A_1]$  or  $[I'_{20}A'_1]$ .

In the following summary we replace the orthogonality-condition (10) by a proportion.

**Theorem 4.** *Under*

$$c\alpha_1 : c\delta_1 : c\beta_2 = c\gamma_1 : c\beta_1 : c\gamma_2, \quad \alpha_2 = \beta_1 \quad \text{and} \quad \delta_2 = -\delta_1$$

the transmission  $\varphi_1 \mapsto \varphi_3$  (Fig. 5a) depends only on the tangents of  $\alpha_1$ ,  $\delta_1$  and  $\beta_2$ . Hence, any other choice of angles  $\alpha'_1, \dots, \delta'_2$  obeying these conditions and eq. (12) gives the same transmission and therefore a flexible Kokotsakis mesh of the orthogonal type IV.

Fig. 6 shows two different decompositions of such a transmission. The underlying overconstrained spherical linkage is a composition of two spherical Dixon-mechanisms (see, e.g., Stachel, 1997). At these mechanisms the bars form a bipartite graph and the knots are moving on two orthogonal great circles.

#### 4.3. A new family of flexible Kokotsakis meshes

Now we specify the second four-bar as mirror of the first one after reflection in an angle bisector at  $I_{20}$  (see Fig. 5b). Depending on the choice of the bisector, this implies

$$(\alpha_2, \beta_2, \gamma_2, \delta_2) = (\delta_1, \pm\gamma_1, |\alpha_1|, -\beta_1) \quad \text{or} \quad (-\delta_1, \pm\gamma_1, |\alpha_1|, \beta_1). \quad (13)$$

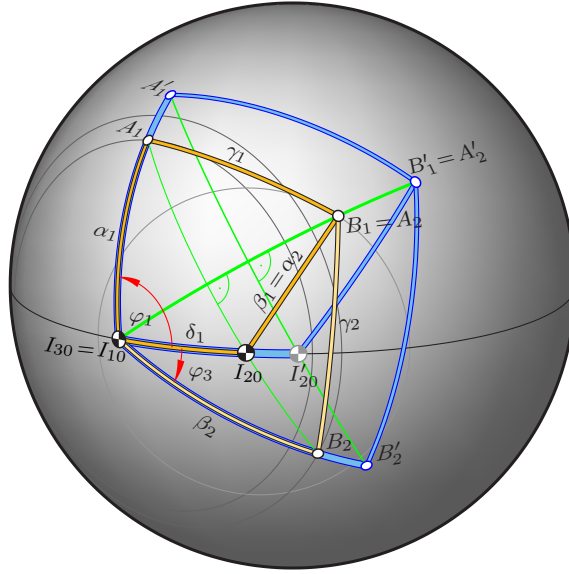


Figure 6: Spherical image of the orthogonal type IV

Angle  $\psi_1$ , previously opposite to the input angle  $\varphi_1$ , becomes the output angle, or more precisely,  $\varphi_3$  equals  $\pm\psi_1$  or  $\pm(\psi_1 - \pi)$ .

However, according to the 4-4-correspondance between  $A_1$  and  $B_2$  there are still two other solutions for  $\varphi_3$ . The corresponding positions of  $B_2$  are mirrors with respect to  $[I_{30}A_2]$ . Hence, the 4-4-correspondance is reducible, and one component is expressed by eq. (7), i.e.,  $c\varphi_3 = \pm(k_1 + l_1c\varphi_1)$ . The sign depends on the choice of the angle bisector at  $I_{20}$ .

As already noted in Section 2.2, there are other four-bars with lengths  $\alpha'_1, \dots, \delta'_1$  which produce the same transmission, i.e., with constants  $k'_1 = \pm k_1$ ,  $l'_1 = \pm l_1$  by (8) and the same center  $I'_{30} = I_{30}$  (Fig. 7). We summarize:

**Theorem 5.** *For the composition of any four-bar  $(\alpha_1, \dots, \delta_1)$  and its mirror obeying (13) the 4-4-correspondance between  $A_1$  and  $B_2$  splits. For one component the cosines of  $\varphi_1$  and  $\varphi_3$  are linearly related. This transmission is shared by other compositions obeying the conditions*

$$\delta_1 + \delta_2 = \delta'_1 + \delta'_2 \pmod{2\pi}$$

and

$$s\alpha_1 s\delta_1 : s\beta_1 s\gamma_1 : (c\alpha_1 c\delta_1 - c\beta_1 c\gamma_1) = s\alpha'_1 s\delta'_1 : \pm s\beta'_1 s\gamma'_1 : (c\alpha'_1 c\delta'_1 - c\beta'_1 c\gamma'_1).$$

The twofold decomposition results in an overconstrained spherical linkage (Fig. 7), which has some properties of so-called *focal mechanisms* in the plane (see, e.g., Wunderlich, 1968). How can the corresponding Kokotsakis mesh be characterized?

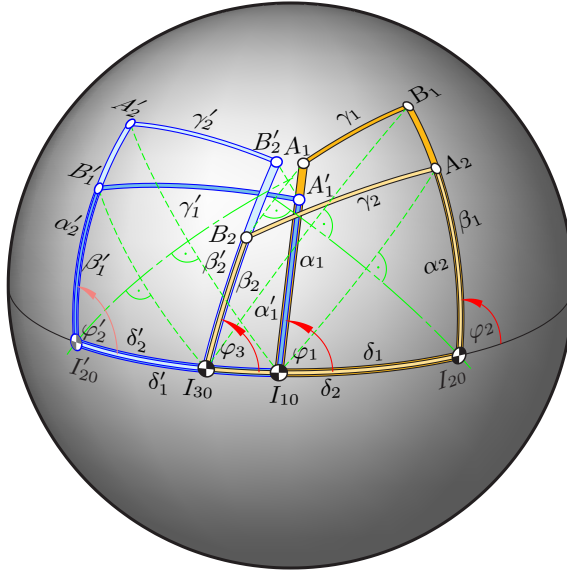


Figure 7: Line-symmetric type V: Two different decompositions of the transmission  $\varphi_1 \rightarrow \varphi_3$

When at the spherical image the four-bars  $I_{10}I_{20}B_1A_1$  and  $I_{20}I_{30}B_2A_2$  arise from each other by reflection in an angle-bisector, then the corresponding preimages, the pyramids with apices  $V_1$  and  $V_2$  are symmetric with respect to a line. This axis of symmetry is perpendicular to  $I_{20}$  and located in a plane bisecting the adjacent planes in  $\Sigma_2$  and  $\Sigma_0$  (compare Fig. 2a). Analogously, the pyramids at  $V_1'$  and  $V_2'$  are line-symmetric. This is why for this new **type V** the name **line-symmetric** is proposed though the symmetry is not global.

**Corollary 6.** *A Kokotsakis mesh with mutually line-symmetric pyramids at  $V_1$  and  $V_2$  as well as at  $V_1'$  and  $V_2'$ , which additionally obeys the conditions listed in Theorem 5, is continuously flexible.*

Kokotsakis' example of a flexible tessellation with convex quadrangles (Kokotsakis, 1932, Fig. 15) is a particular case of this type V, but there also the pyramids at  $V_1$  and  $V_1'$  are mutually line-symmetric as well as that at  $V_2$  and  $V_2'$  (see Stachel, 2009). Here the signed angles fulfill the following conditions:

$$\begin{aligned} \alpha_1 + \beta_1 + \gamma_1 + \delta_1 &= 2\pi, & (\alpha_2, \beta_2, \gamma_2, \delta_2) &= (-\delta_1, \gamma_1, \alpha_1, \beta_1), \\ (\alpha_1', \beta_1', \gamma_1', \delta_1') &= (-\delta_1, \gamma_1, \beta_1, -\alpha_1), & (\alpha_2', \beta_2', \gamma_2', \delta_2') &= (-\alpha_1, -\beta_1, \delta_1, -\gamma_1). \end{aligned}$$

The composition of two linear functions of type (7) is still a linear function. Therefore we can iterate and use  $k$  pairs of symmetric four-bars on the right-hand side and  $l$  pairs on the left-hand side. As long as they share the resulting linear function and the resulting center of rotation, the complete spherical linkage is continuously flexible. The corresponding preimage is a *flexible Kokotsakis mesh* with even  $n = 2(k + l)$ .

Finally it should be mentioned that for given  $\alpha_1, \beta_1, \gamma_1, \delta_1$ , and  $\beta'_1$  the remaining angles  $\alpha'_1, \gamma'_1, \delta'_1$  obeying the conditions of Theorem 5 can be computed. For  $\beta'_1$  sufficiently close to  $\beta_1$  real solutions must exist (compare Fig. 7).

## References

- Bricard, R., 1897. Mémoire sur la théorie de l'octaèdre articulé. *J. math. pur. appl.*, Liouville 3, 113–148.
- Bobenko, A.I., Hoffmann, T., Schief, W.K., 2008. On the Integrability of Infinitesimal and Finite Deformations of Polyhedral Surfaces. In: Bobenko et al. (eds.), 2008, *Discrete Differential Geometry, Series: Oberwolfach Seminars 38*, pp. 67–93.
- Karpenkov, O.N., 2008. On the flexibility of Kokotsakis meshes. [arXiv:0812.3050v1](https://arxiv.org/abs/0812.3050v1) [mathDG], 16Dec2008.
- Kokotsakis, A., 1932. Über bewegliche Polyeder. *Math. Ann.* 107, 627–647.
- Piekarski, M., 2000. Constructional Solutions for Two-Way-Fold-Deployable Space Trusses. In: Pellegrino, S., Guest, S.D. (eds.), *Deployable Structures: Theory and Applications*, Kluwer Academic Publ., pp. 301–310.
- Pottmann, H., Liu, Y., Wallner, J., Bobenko, A., Wang, W., 2007. Geometry of Multi-layer Freeform Structures for Architecture. *ACM Trans. Graphics* 26(3), SIGGRAPH 2007.
- Sauer, R., 1970. *Differenzengeometrie*. Springer-Verlag, Berlin/Heidelberg.
- Sauer, R., Graf, H., 1931. Über Flächenverbiegung in Analogie zur Verknickung offener Facettenfläche. *Math. Ann.* 105, 499–535.
- Stachel, H., 2000. Das Gleichlauf-Kugelgelenk – ein Beispiel zum anwendungsorientierten Unterricht aus Darstellender Geometrie. *Proc. SDG Symposium Darstellende Geometrie, Dresden 2000* (ISBN 3-86005-258-6), 151–156.
- Stachel, H., 1987. Zur Einzigkeit der Bricardschen Oktaeder. *J. Geom.* 28, 41–56.
- Stachel, H., 1997. Euclidean line geometry and kinematics in the 3-space. In: Artémiadis, N.K., Stephanidis N.K. (eds.): *Proc. 4th Internat. Congress of Geometry, Thessaloniki 1996* (ISBN 960-7425-11-1), pp. 380–391.
- Stachel, H., 2009. Remarks on Miura-ori, a Japanese Folding Method. *Acta Technica Napocensis, Ser. Applied Mathematics and Mechanics* 52, Vol. Ia, 245–248.
- Wegner, B., 1984. On the projective invariance of shaky structures in Euclidean space. *Acta Mech.* 53, 163–171.
- Wunderlich, W., 1968. On Burmester's focal mechanism and Hart's straight-line motion. *J. Mechanism* 3, 79–86.